Turbulent film condensation in a vertical tube in presence of non condensable gas

Y. Belkassmi, K. Gueraoui, N. Hassanain, A. Elbouzidi

Team of vapour gas in fluid mechanics and environment, LPT, URAC 13 Faculty of sciences, Mohammed V University, Rabat-Agdal B.P. 1014, Rabat, Morocco

y.belkassmi@gmail.com

Team of vapour gas in fluid mechanics and environment, LPT, URAC 13 Faculty of sciences, Mohammed V University, Rabat-Agdal B.P. 1014, Rabat, Morocco

Department of mechanical engineering, Ottawa University, Canada

kgueraoui@yahoo.fr

Team of magnetic materials and applications, LPM, 4 Avenue Ibn Battouta Faculty of sciences, Mohammed V University, Rabat-Agdal B.P. 1014 RP, Rabat, Morocco

najem.hassanain@gmail.com

Team thermodynamic energy, Faculty of sciences, Mohammed V University, Rabat-Agdal B.P. 1014, Rabat, Maroc

Elbouzidi.abdellah@gmail.com

ABSTRACT

This paper presents the simulation of the condensation of methanol vapour in the presence of non-condensable gas in turbulent flows in a vertical tube. The liquid and gas stream are approached by two coupled turbulent boundary layer. For solving the coupled governing equations for liquid film and gas flow together with the interfacial matching conditions an implicit finite difference method is employed. The effect of the influencing parameters are studied so the effect of inlet Reynolds number, the effect of temperature gradient, mass fraction are illustrated. The numerical results demonstrate that an important concentration of no-condensable gas reduces the heat transfer coefficient and film thickness considerably. The local heat flux and film thickness increase as tube surface temperature decreases at any bulk concentration of non-condensable gas. Moreover, inlet velocity increases as film thickness decreases and heat flux increases.

Keywords

Condensation; Heat and mass transfers; mixed convection; turbulent flow; Vertical tube; Methanol vapour.

Council for Innovative Research

Peer Review Research Publishing System

1. INTRODUCTION

Condensation of frigorific vapour in the presence of non-condensable gases has many applications such as air conditioning, electricity generation, refrigeration, reactor safety, aerospace, desalination and some heat exchangers. From the literature we report a several studies in the laminar case [1-7] of condensation in a vertical tube and other studies in the turbulent case [8-13]. Belkassmi et al [2] presented a numerical study of film condensation by forced convection in a vertical tube; they studied the effect of some parameter influence on the phenomenon of condensation in the laminar case. Revankar and Oh [3] was study the complete condensation of saturated vapor in laminar liquid film in a vertical tube isothermal wall, the study is theoretical and the model elaborate have considered the evolution of the shear stresses at the interface and profiles of liquid and vapor velocity.

A numerical study of laminar mixed convection condensation of steam in the presence of non-condensable gases was performed by Chin et al. [4] the model adopted is based on the equations of two-dimensional two-phase boundary layer by considering the inertia terms, Convection and constraints shear at the interface and variable physical properties. The thickness of the liquid film is calculated from the thermal balance at the interface. In the same context Oh [5] has made a study, the equations of the two-phase boundary layer systems are solved by the finite difference method for laminar liquid film and finite volume for the turbulent steam.

Louahlia and Panday [8] have studied numerically the film condensation between two horizontal plates by forced convection of refrigerants R134 and R123 and their mixture. The coupled equations of masse conservation, the momentum equation, species and energy are applied in two phases using the boundary layer models. Panday [9] conducted a numerical study of turbulent film condensation inside a vertical tube the walls are isothermal, the saturated vapour of R123 then the mixture of R134a-R123 are studied. Wang and Tu [10] have developed a model for analyzing the effect of a non-condensable gas in film condensation of gas-vapor mixture in turbulent flow in a vertical tube. They noticed that the reduction of heat transfer due to the non-condensable gas was more significant at low pressure and at low Reynolds number of the mixture.

The problem of condensation of methanol vapour in the presence of non-condensable gas (air) in turbulent flow along of a vertical tube is tackled theoretically. The walls are isotherm, the condensate film on the wall of the pipe is assumed to be a thin film in turbulent flow, the heat and mass transfers in the liquid and vapor phase are governed respectively by classical stream, and forced convection equations, transfers equations are linked at the liquid vapor interface by the continuity of the shear stress and the heat flux densities and by the heat flux density through the wall of the tube. The equations are discredited by the finite difference method and solved by Tomas algorithms.

2. ANALYSIS

Fig.1 shows a schematic of the physical model considered for the condensation process with defined coordinate systems. We consider a forced convection vapor mixture flow downward inside a vertical tube of (L) height and (d) with. The temperature of the wall is maintained at T_{wall}, and the mixture enters the tube with a uniform velocity u_0, uniform temperature T_0, uniform pressure P_0 and uniform gas mass fraction W_0. The following assumptions were made in the development of governing equation:
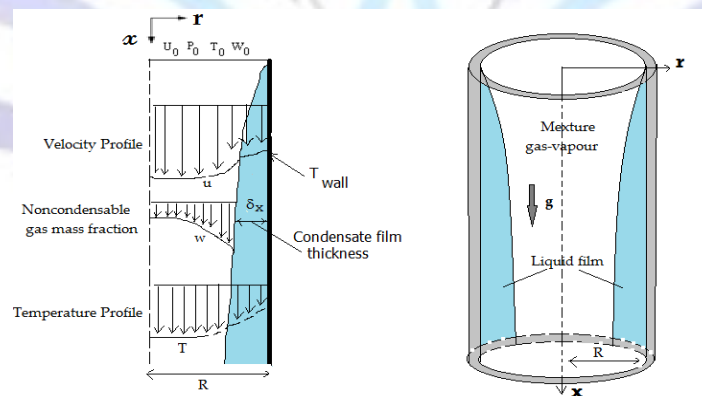

Fig.1 Physical model for vertical tube condenser

- The liquid and gas flows are turbulent and the flow is tow-dimensional.

- The condensate film is impermeable to incondensable gas.

- Humid air is an ideal mixture of methanol vapor it is considered a perfect gas.

- The Soret and Duffour effects are ignored, and the effect of the superficial tension is neglected.

- The gas-liquid interface is in the thermodynamic equilibrium.

The following equations are written for the boundary layers.

2.1 Liquid film equations
Continuity equation

$$\partial(\rho_l u_l)/\partial x + (1/r)\partial(r\rho_l v_l)/\partial r = 0 \qquad (1)$$

Momentum equation

$$\partial(\rho_l u_l u_l)/\partial x + \partial(u_l \rho_l v_l)/\partial r = -dP/dx + (1/r)\partial/\partial r[(\mu_l + \mu_{tl})\partial u_l/\partial r] + \rho_l.g \qquad (2)$$

Energy equation

$$\partial(u_l\rho_l C_{Pl}T_l)/\partial x + \partial(v_l\rho_l C_{Pl}T_l)/\partial r = (1/r)\partial/\partial r[r(\lambda_l + \lambda_{tl})\partial T_l/\partial r]$$
$$(3)$$

2.2 Gas flow equations
Continuity equation

$$\partial(\rho_G u_G)/\partial x + (1/r)\partial(r\rho_G v_G)/\partial r = 0 \qquad (4)$$

Momentum equation

$$\partial(\rho_G u_G u_G)/\partial x + \partial(\rho_G u_G v_G)/\partial r = -dP/dx + (1/r)\partial(r(\mu_G + \mu_{tG})\partial u_G/\partial r)/\partial r + \rho_G.g \qquad (5)$$

Energy equation

$$\partial(\rho_G C_{PG} u_G T_G)/\partial x + \partial(\rho_G C_{PG} v_G T_G)/\partial r = (1/r)\partial/\partial r[r(\lambda_G + \lambda_{tG})\partial T_G/\partial r] \qquad (6)$$

Species equation

$$\partial(\rho_G u_G w_G)/\partial x + \partial(\rho_G v_G w_G)/\partial r = (1/r)\partial[r\rho_G(D_G + D_{tG})\partial w/\partial r]/\partial r \qquad (7)$$

2.3 Turbulence modeling
Liquid film:

As outlined in Yih and Liu [12] a modified Van Driest eddy viscosity model proposed by Yih and Liu was used to simulate the turbulence in the liquid film. Similar turbulence modeless was also used to simulate the heat transfer across a turbulent falling film. The turbulent eddy viscosity is given by:

$$\mu_{Lt}/\mu_L = -0.5 + 0.5\left\{1 + 0.64 y^{+2}(\tau/\tau_w) \times \left[1 - exp(-y^+(\tau/\tau_w)^{1/2}/A^+)\right]^2 \times f^2\right\}^{1/2}$$

For: $\quad 0.6 < (R - r/\delta) < 1.0 \quad$ *where* $\quad f = exp\left[-1.66\left(1 - \left(^{\tau}/_{\tau_w}\right)\right)\right], \quad y^+ = (R - r)u_*/v, \quad A^+ = 25.1$

For : $\quad (R - r)/\delta_x < 0.6$ the turbulence eddy viscosity for the liquid film was taken as constant an equal to its value at $(R - r)/\delta_x = 0.6$. The turbulent conductivity λ_{Lt} can then be obtained by introducing the turbulent Prandtl number Pr_{Lt} so $\lambda_{Lt} = \mu_{Lt}.C_{pL}/Pr_t$, where the turbulent Prandtl number is evaluated from Cebeci and Smith [14].

Gas flow : The realizable $\mathrm{k} - \varepsilon$ model was used to model turbulence in the present simulation in the gas flow, a low Reynolds number model in evaporation case is adopted [15 , 16]. The governing equation for the turbulent kinetic energy k and the dissipation rate ε are,

$k - transport$

$$\rho_G u\frac{\partial k}{\partial x} + \rho_G v\frac{\partial k}{\partial r} = \frac{1}{r}\frac{\partial}{\partial r}\left[r\left(\mu_G + \frac{\mu_{tG}}{\sigma_k}\right)\frac{\partial k}{\partial r}\right] + \mu_{Gt}\left(\frac{\partial u_G}{\partial r}\right)^2 - \rho_G(\tilde{\varepsilon} + D_v)$$

$\varepsilon - transport$

$$\rho_G u \frac{\partial \tilde{\varepsilon}}{\partial x} + \rho_G v \frac{\partial \tilde{\varepsilon}}{\partial r} = \frac{1}{r} \frac{\partial}{\partial r} \left[r \left(\mu_G + \frac{\mu_{tG}}{\sigma_\varepsilon} \right) \frac{\partial \tilde{\varepsilon}}{\partial r} \right] + C_{\varepsilon 1} f_1 \frac{\tilde{\varepsilon}}{k} \mu_{Gt} \left(\frac{\partial u_G}{\partial r} \right)^2$$

$$- \rho_G C_{\varepsilon 2} f_2 \frac{\tilde{\varepsilon}^2}{k} + \frac{2 \mu_G \mu_{Gt}}{\rho_G} \left(\frac{\partial^2 u_G}{\partial r^2} \right)^2$$

The model constants and function are,

$$f_1 = 1 \quad , \quad f_2 = 1 - 0.3 \, exp\left(-Re_t{}^2\right) \quad , \quad f_\mu = exp(-3.4/(1 + Re_t/50)^2)$$

$$\tilde{\varepsilon} = \varepsilon - D_\varepsilon , \quad D_\varepsilon = 2v \left(\frac{\partial k^{1/2}}{\partial r} \right)^2$$

c_ε	c_k	$c_{\varepsilon 2}$	$c_{\varepsilon 1}$	c_μ
1.3	1.0	1.92	1.44	0.99

2.4 Boundary Conditions

The boundary conditions of these marching type problems are:

$$x = 0 \quad , \quad u_g = u_0 \quad , \quad T_g = T_0 \quad , \quad w = w_0$$

$$P = P_0, \quad k_0 = 3(I_0 u_g)^2/2 \quad , \tilde{\varepsilon}_0 = c_\mu k_0{}^{3/2}/\kappa R \quad , \quad w = w_0$$

$$r = R \quad , \quad u_l = v_l = 0 \quad , \quad T = T_w$$

$$r = 0 \, , \, v_g = 0 \, , \, \partial u_g/\partial r = 0 \, , \, \partial T_g/\partial r = 0$$

$$\partial w/\partial r = 0 \quad \partial k/\partial r = \partial \tilde{\varepsilon}/\partial r = 0$$

The solution from the liquid side and gas side satisfy the following interfacial ($r = (R - \delta_x)$) matching conditions:

✓   continuities of velocity and temperature:

✓
$$u_I(x) = u_{g,I} = u_{l,I}, \qquad T_I(x) = T_{g,I} = T_{l,I} \tag{11}$$

✓   Continuity of shear stress:
$$\tau_I = (\mu_G + \mu_{tG})[\partial u/\partial r]|_{G,I} = (\mu_l + \mu_{lt})[\partial u/\partial r]|_{l,I} \tag{12}$$

✓   Velocity of air vapour mixture at the interface. The transverse velocity component of the air vapour mixture at the interface is deduced by assuming the interface to be semi-permeable, that is the solubility of air into the liquid is negligibly, the velocity at interface can be calculated by :
$$v_I = -[(D_G - D_{Gt})/(1 - w_I)]\partial w/\partial r \tag{14}$$

✓   Heat balance at the interface :
$$\lambda_l(\partial T_l/\partial r)_I = \lambda_g(\partial T_G/\partial r)_I - h_{fg}\dot{m}_I \tag{15}$$

in which h_{fg} is the latent heat of condensation, and $\dot{m}_I$ the condensate generation rate.

✓   The mass fraction at the interface can be calculated using:
$$w_I = \frac{M_v P_{v,I}}{M_a(P_G - P_{v,I}) + M_v P_{v,I}} \tag{16}$$

Where P and $P_{v,I}$ are the total pressure and the vapour pressure at the interface, respectively. M_a and M_v are the molecular heights of air and methanol vapor respectively. The thermodynamic proprieties of the liquid film and gas are considered variable.

2.5 Heat and mass transfer parameters

The total interfacial heat flux:

The local Nusselt number along the interface gas-liquid is defined as:

$$Nu_x = \frac{h_T D_h}{\lambda_{tG}} = \frac{q_I D_h}{\lambda_{tG}(T_I - T_b)} = \frac{\left(\lambda_{tG} \dfrac{\partial T_G}{\partial r} \bigg|_I - \dot{m}_I h_{fg} \right) D_h}{\lambda_{tG}(T_I - T_b)} \tag{17}$$

So the total convective heat transfer rate from the film interface to the gas stream can be expressed as follows:

$$q_T = q_{s,I} + q_{L,I} = (\lambda_G + \lambda_{tG})\partial T_G/\partial r - h_{fg}\dot{m}_I \tag{18}$$

The local Sherwood number:

We defended the local Sherwood number relief at the mass transfer coefficient and the diffusive mass flux as:

$$Sh_x = \frac{h_{M,x} d_h}{\lambda_G D_v} \qquad (19)$$

The cumulate rate of condensation:

$$M_r = \frac{\int_0^x \dot{m}.dx}{M_0} \qquad (20)$$

Where the $\dot{m}$ is the condensate mass rate and $\dot{M}_0$ is the mass debit of gas at the inlet of tub, and at every axial location, the overall mass balance in the gas flow and liquid film should be satisfied.

2. NUMERICAL METHODE

The conjugate problem defined by the parabolic systems, equations (1)-(7) and those of turbulence, with the appropriate boundary conditions are solved by a finite difference numerical scheme. Each system of the matrix equation which can be solved by the Thomas algorithm [17]. The correction of the pressure gradient and axial velocity profile at each axial station in order to satisfy the global mass flow constraint is achieved using a method proposed by Raithby and Schneider1979 [18]. The discrete equations are resolved line by line from the inlet to the outlet of the tube since flows under consideration are a boundary layer type.

Several grid sizes have been tested to ensure that the results are grid independent Grid independence tests were carried out by comparing the total heat transfer for different values of I, J and K. In light of those results all further calculations were performed with the $131 \times (81 \times 31)$ grids this is an optimums mesh of this study. So the grid distribution adopted in this study consists of 31, 81, and 131 nodes, respectively, in the transverse direction of the liquid region, transverse direction of the gas region and in the axial direction.

In other way, we transformed the Cartesian z coordinates into η coordinate system in this study, such that the centre line is at $\eta = 0$, the liquid-mixture interface is at $\eta = 1$, and the wall is at $\eta = 2$. The equations that relate the η coordinate system to the r coordinate system are:

$$\eta_L = 2 - (R - r)/\delta \quad \text{for} \qquad R - \delta \leq r \leq R \qquad (21)$$

And
$$\eta_G = r/(R - \delta) \quad \text{for} \qquad 0 \leq r \leq R - \delta \qquad (22)$$

A sensitivity analysis of the numerical model for the dimension of mesh was conducted to determine the optimal mesh. Some dimensions of grids were used to calculate the Nusselt number defined by the equation (17) as it has found that is the most severe test. The calculate of the error for grid shows that the error does not exceed 5% in the case (NI = 141, NJ = 81, NL = 31), consequently the grid 131 × 81 × 31 mesh was used for following our study. The table below shows the comparing number of local Nusselt at the interface for different mesh.

$$P_0 = 1\text{atm} \ , T_0 = 40\text{C}° \ , T_0 = 20\text{C}°, \quad Re = 500 \quad , W_0 = 0.8$$

x/d	NI=131,NJ=51,NL=21	NI=131,NJ=81,NL=31	NI=131,NJ=81,NL=21
1.51189954	142.88570645	150.32025362	149.99433678
4.58120674	91.88363011	95.00242783	95.10454844
20.87831547	57.87359033	59.08683097	59.11598383
58.76602663	40.30052290	40.75164816	40.82998208
102.45972984	31.47931832	31.65063657	31.77498553
152.21245169	25.16940859	25.21354221	25.34368250
230.23628428	18.82011596	18.80087019	18.90553089

x/d	NI=141,NJ=51,NL=21	NI=141,NJ=81,NL=31	NI=141,NJ=81,NL=21
1.32139812	149.55703634	157.78633133	157.43786590
5.36540618	87.60830443	90.49476060	90.59076548
21.27040609	57.66774546	58.87400105	58.90457111
60.72183139	39.84096119	40.27516702	40.35748360
103.18802770	31.40648816	31.57608576	31.70142775
152.16183269	25.19816792	25.24304252	25.37356488
232.45766297	18.69056538	18.67101621	18.77494119

4. RESULTS AND DISSCUSSION

The figure 2, shows the profiles of radial velocities for different temperature gradient in the two phases, the radial variations of these values in the liquid phase are lower than in the gas mixture. In the case of a vertical tube, the velocity of the gas mixture is maximum on the axis of the tube $\eta = 0$ and minimum at the interface $\eta = 1$. The condensate velocity profiles in the liquid film gradually increase along of tube because of his entrainment by the gas stream and his gravity; these values are lower than those of the gas mixture, it due to his high viscosity. In other the values of velocity are important for high temperature gradient $\Delta T = 35\,°C$ relatively in gas mixture. The figures 3, 5 illustrate the effect of Reynolds number respectively on the Sherwood number sh then on the film thickness of the condensate. It shows that the thickness is greater with increasing Reynolds number thing which we see in figure.3 this means that the transfer of heat and mass are more effective in forced convection. The figure 4 shows the affect of the Reynolds turbulent number on the kinetic energy; we chose different values which includes the two regimes laminar and turbulent. We maintaining constant the following parameters, $P_0 = 1\,atm$, $Re_0 = 3500$, $W_0 = 0.5$ and we study the effect of the temperature difference ΔT between the wall and the gas mixture air-steam of methanol saturated.
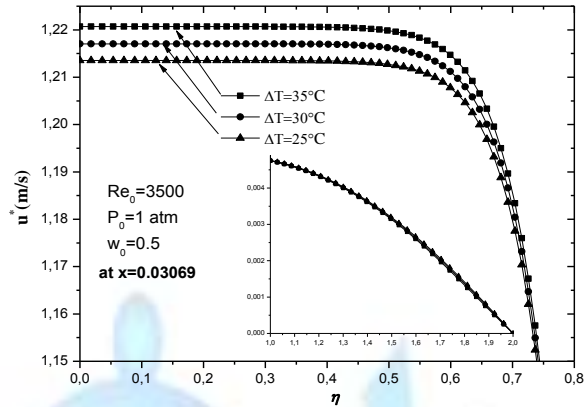
A inlet temperature T_0 fixed the values adopted are $\Delta T = 25\,°C, 30\,°C, 35\,°C$ the results shown in Figures 2,6,7,8 show that, for the same values of input debit, P_0 pressure and w_0 vapor concentration, the values of film thickness, liquid flow and heat flux do not converge to the same limit at the end of condensation, the increase of ΔT causes a decrease in temperature parietal, the rate of vapor in the mixture, consequently the increase of the difference between the vapor mass fractions $(w_0 - w_b)$. This which leads to increased temperature gradients, vapour concentration and the rate of condensation. It follows a significant increase of the liquid mass flow rate (Fig.6) and the heat flux to the wall (Fig.7).
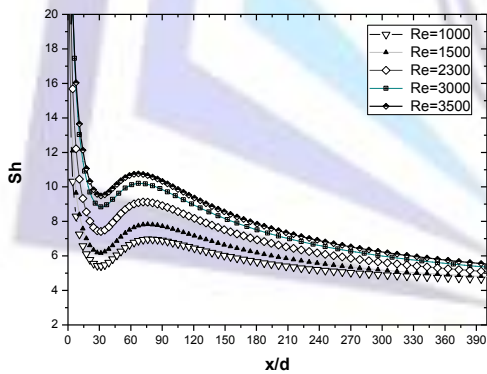
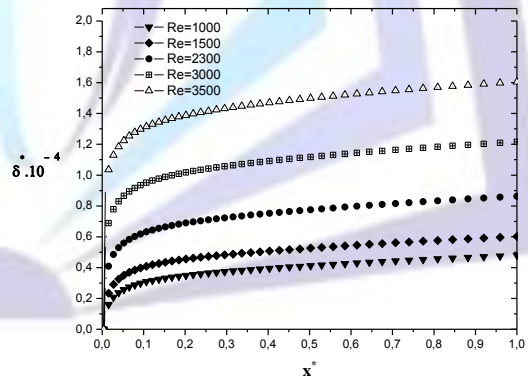**Figure.3 Effect of Reynolds number on the evolution of the Sherwood number.**

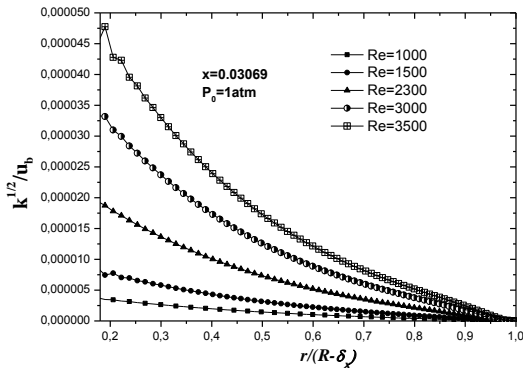**Figure.5 Effect of Reynolds number on the evolution of the thickness of liquid film.**

Figure.4 Effect of Reynolds number on the evolution of the turbulent kinetic energy.
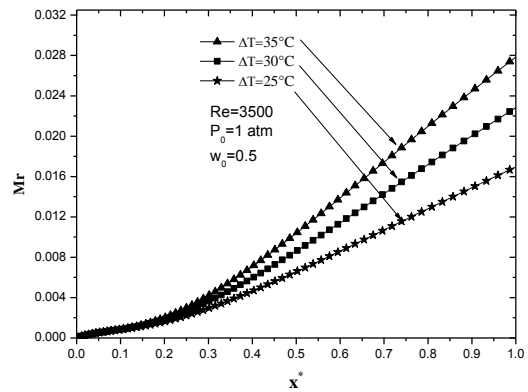

Figure.6 Effect of Reynolds number on the evolution of the rate.

The fig.9 show the thickness of condensate it show that it increase with the tube long it increase also with the important values of mass fraction. This can be explained by the fact that the non condensable gas accumulating near to interface which limits the heat transfer and consequently the deprivation of methanol vapour condensation. On the other hand we see that for the fraction values of 40% the thickness is relatively pronounced because the thermal resistance near to interface is relatively in regression comparing with 80% case.
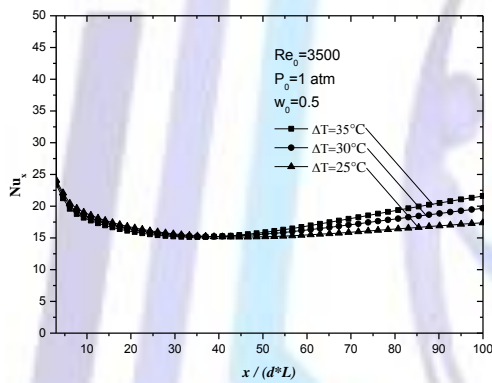

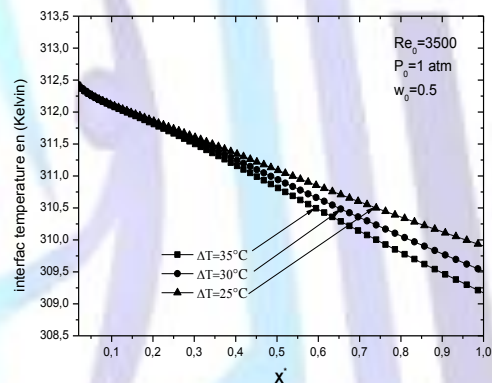**Figure.7 Effect of temperature difference on the evolution of the Nusselt number.**

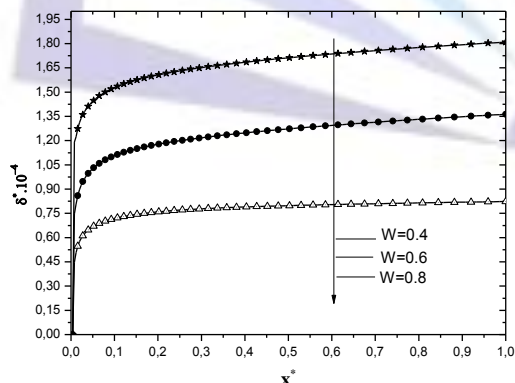**Figure.8 Effect of temperature difference on the evolution of the interfacial temperature.**

Figure.9 Effect of mass fraction on the evolution of the thickness of liquid film.
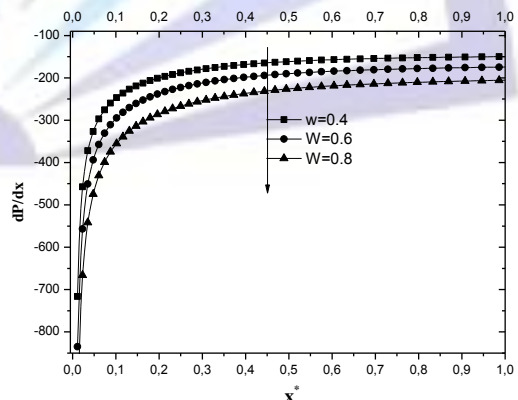

Figure.10 Axial pressure gradient with effect of mass fraction

In Figure 10 the variations of axial pressure gradients are shown for these three cases of mass fraction. Most of the pressure gradient is predicted from inlet of the condensation tube to $x^* = 0.3$. From Equation (2), it can be seen that the vapor pressure gradient is affected by changes in the momentum flux as well as by the interfacial shear (the gravitational pressure gradient is considered to be negligible). The momentum change of the vapor flow tends to increase the pressure in the flow as the condensation occurs at the wall, while the interfacial stress tends to cause a decrease in pressure on other the pressure gradient is affected by the local condensation heat flux, then the inlet large pressure gradient indicates large condensation.

5. Conclusion

The contribution to the heat and mass transfer in vertical tube tow dimensional for the air methanol vapour mixture in case of turbulent is the mean objective of our study. A theoretical model is developed in the turbulent case in the presence of non-condensable gas using a finite difference. The conservation equation for mass, momentum, energy, and species concentration are developed. The resultants presented clearly that the condensation heat transfer coefficients and the rate of condensation decreases considerably in the presence of non-condensable gas in high percentage. The numerical results of the present theoretical study agree satisfactorily with the data available in literature.

REFERENCES

[1] Siow, E.C., 2001, Numerical solution of two-phase model for laminar film condensation of vapour-gas mixtures in channels. M.Sc. thesis, University of Manitoba, Winnipeg, Manitoba.

[2] Belkassmi, Y., Gueraoui, K., Hassanin, N., 2012, Numerical study in condensing of methanol vapor in a vertical tube by mixed convection in the presence of non-condensable Gas. Adv Studies Theor Phys. 6, 1065 – 1076.

[3] S. Oh, S. T. Revankar "Analysis of the complete condensation in a vertical tube passive condenser", International Communications in Heat and Mass Transfer 32, pp. 716–727, 2005.

[4] Y.S. Chin, S.J. Ormiston, H.M. Soliman ''Two-phase boundary-layer model for laminar mixed-convection condensation with a non condensable gas on inclined plates", Heat and Mass Transfer 34, pp. 271–277, 1998.

[5] S. Oh "Turbulent Heat and Mass Transfer in a Vertical Condenser Tube", Fall Semester ME605 Convective Heat and Mass Transfer, Project Report,2003.

[6] Y. El hammami M. Feddaoui T. Mediouni R. Mir A. Mir. Étude numérique de la condensation en film par convection mixte a l'interieur d'un canal a paroi poreuse. Revue International d'Héliotechnique, 42 :18–24, 2010.

[7] Y. El Hammami M. Feddaoui T. Mediouni A. Mir. Numerical study in condensing a liquid refrigerant (r134a) film along a vertical channel. International symposium on convective heat and mass transfer in sustainable energy Hammamet Tunisia.,2 :426–429, 2009.

[8] H. Louahlia, P.K. Panday Transfert thermique pour la condensation du R123, du R134a et de leurs mélanges en écoulement forcé entre deux plaques planes horizontales: Etude numérique, Rev. Gén. Therm., Vol. 35, pp.615–624, 1996.

[9] P.K. Panday Two-dimensional turbulent film condensation of vapours flowing inside a vertical tube and between parallel plates: a numerical approach, Int. Journal of Refrigeration 26, pp. 492-503, 2003.

[10] C.Y. Wang, C.J. Tu "Effects of non-condensable gas on laminar film condensation in a vertical tube", International Journal of Heat and Mass Transfer 31, No 11, 2339-2345, 1988.

[11] Ormiston, S.J., Groff, M.K., Soliman, H.M., 2007, Numerical solution of film condensation from turbulent flow of vapor–gas mixtures in vertical tubes. International Journal of Heat and Mass Transfer 50, 3899–3912.

[12] S. Yih, J. Liu(1983), "Prediction of heat transfer in turbulent falling liquid films with or without interfacial shear", AIChE Journal, vol. 29, pp. 903-909.

[13] A. Wurster, Discussion, Trans. Am. Inst. Chem. Eng. 38 (1942) 464–468.

[14] T. Cebeci, A. M. O. Smith(1970), "A finite difference method for calculating compressible and turbulent boundary layers", J. Basic Engineering. Trans ASME. vol. 92, pp. 523-535.

[15] B. E. Launder, B. I. Sharma (1974), "Application of the energy-dissipation of turbulence to calculation of low Reynolds number flow near a spinning disc" Lett. Heat Mass transfer, vol. 1, pp. 131-138.

[16] M. Feddaoui, H. Meftah, A. Mir, The numerical computation of the evaporative cooling of falling water film in turbulent mixed convection inside a vertical tube, Int. J. Heat Mass Transfer 33 (2006) 917–927.

[17] Patankar S.V. [1980] "Numerical Heat Transfer and Fluid Flow". Hemisphere/Mc Graw Hill. New York, Chap.6.

[18] Raithby, G. D.; Schneider, G. E. [1979] Numerical solutions of problems in incompressible fluid flow: treatment of the velocity-pressure coupling. Numer. Heat. Tran., Vol. 2, pp. 417-440.

Symbol	Description	Units	Symbol	Description	Units
c_p	Specific heat	$j \cdot kg^{-1} \cdot K^{-1}$	δ	Thickness of condensate layer	m
D	Mass diffusivity	$m^2 s^{-1}$	δ^*	Dimensionless film thickness	
d	Tube half width	m	λ	Thermal conductivity	$W.m^{-1}K$
g	Gravitational acceleration	$m.s^{-2}$	η	Transformed coordinate defined by eqs (20, 21)	
h_{fg}	Latent heat of condensation	$j \cdot kg^{-1}$	μ	Dynamic viscosity	$kg \cdot s^{-1}m^{-1}$
h_T	Local heat transfer coefficient	$W.m^{-2}K^{-1}$	ρ	Mass density	$kg\ m^{-3}$
$\dot{m}_0$	Mass flow rate	$kg.m^{-1}.s^{-1}$	I	liquid-gas interface indicate	
q_t	Total heat flux	$W.m^{-2}$	0	Zero, condition at inlet	
q_{LI}	Latent heat flux	$W.m^{-2}$	L	Liquid index / Length	
q_{sI}	Sensible heat flux	$W.m^{-2}$	G	Gas index	
T_0	Inlet temperature	K	W	Wall index	
T^*	Dimensionless temperature $((T - T_{wall})/(T_0 - T_{wall}))$				
u^*	Dimensionless velocity in the y-direction (u/u_0)				
W^*	Dimensionless vapor mass fraction $((W - W_0)/(W_I - W_0))$				
x	Coordinate along the tube				
r	Coordinate normal to the tube				
k	Kinetic energy				
ε	Dissipation rate				